Thermal behaviors of mesocarbon microbeads and physical properties of carbon plates

X. B. HU, B. Y. ZHAO, K. A. HU
State Key Laboratory of Metal Matrix Composites, Shanghai Jiaotong University,
1954 Huashan Road, Shanghai 200030, People's Republic of China
E-mail: Hu_peter@sjtu.edu.cn

Mesophase microbeads are a prominent precursor of carbon artifacts with high density and high strength since the powder has significant self-sintering ability. The formation of sintering bridges as a consequence of the liquid-phase sintering at approximately 535°C is inferred by thermal analysis. According to thermogravimetric and DSC analyses, the intensive pyrolysis of MCMBs occurs from about 600 to 800°C and releases volatiles thus resulting in remarkable volume shrinkage. In this work, carbonaceous plates without binder are prepared by cold molding from MCMBs with 2.1 of C/H mole ratio and about 12 μm of average particle size, sintered at three different temperatures of 800, 1150 and 1400°C. A relative higher bulk density of 1710 kg/m^3, bending strength of 84 MPa and electrical conductivity of 2.4 S/m are obtained successfully after calcining the plate at 1400°C.
© *2004 Kluwer Academic Publishers*

1. Introduction
Since Honda and Yamada [1] first separated meso-carbon microbeads (MCMBs) from the mesophase pitches, it has been well known that MCMBs are good self-sintering precursors for high density and high strength artifacts of carbon and graphite [2–5]. Their spherical shape, controlled fusibility and packing flexibility are favorable for making high density and high strength artifacts because MCMBs are believed to ensure adequate adhesion among particles within the artifact through partial fusion during heat treatment. Their homogeneous shrinkage will induce minimal defects such as cracks and voids into the artifacts. Thereby, such special carbon artifacts show homogenous density, physical isotropy and good conductivity, and have been utilized as the basic material for semiconductor industry, battery manufacture, nuclear reactors and electric brushes [3].

The procedure to produce carbon artifacts can be classified into two typical categories. The first one uses pulverized coke as filler and pitch as binder, often resulting in porous products of rather low density and insufficient strength, hence baking and impregnation are necessary to be repeated several times. The second one uses self-adhesive carbonaceous grains for binderless molding [5–7]. MCMBs are self-sinterable probably coming from a fraction of molecules of the powders that provide fluidity to the material, commonly called β-resin i.e. *in-situ* binder [8–11].

The physical performances of the resulting carbons strongly depend on the morphology and the thermal behaviors of MCMBs, together with the calcination conditions. Some studies [11–13] have shown that the MCMBs have a lamellar polyaromatic structure with aliphatic, naphthenic side chains and functional groups of hetero atoms which result in plasticity and fusibility. However, only a few studies deal with the thermal behavior of MCMBs in the literature [12, 14, 16]. The analysis shows that the sintering of MCMBs can be divided into at least two quite distinct stages [12]. The first stage is in the lower temperature range around approximately 535°C during which the powder spherules passes through a liquid or at least plastic phase and it can be assumed that the decisive sintering bridges between the particles are formed in this stage, by the mechanism of liquid-phase sintering. However, this liquid-phase sintering is only a transient interim, because the mesophase solidification is continued if heating is continued. Thereafter is the second stage, above the solidification temperature of about 550°C, concomitant with significant shrinkage of the solidified material due to solid phase sintering. But it is believed that intragranular shrinkage is the main cause rather than intergranular shrinkage during liquid-phase sintering [15–18].

In subsequent research it is attempted to explore the thermal behaviors of MCMBs postulated liquid-phase sintering and to examine the effects of different carbonization conditions on physical properties of carbon plates.

2. Experiment
2.1. Materials and thermal behaviors of MCMBs
Mesocarbon microbeads are prepared from coal tar pitch, supplied by Shanghai Shanshan Tech Company. Particle size distribution of MCMBs is within a narrow

range from 8 to 19 μm and average size about 12 μm. The morphology of MCMBs as received is observed through a SEM (JEOL, JSM-840A).

The elemental composition of the MCMBs as received is examined by an element analyzer (2400-2, Perkin Elemer, Germany) and thermogravimetric analysis is performed by a TGA thermal analyzer (Perkin Elmer, Germany) at a rate of 20°C/min heating up to 950°C in nitrogen atmosphere. Differential Scanning Calorimetry (DSC) is carried out in nitrogen atmosphere by a DSC analyzer (DSC 404, Netzsch-Geratebau, Germany) at a heating rate of 10°C/min from 40°C to 1100°C for general analysis and a heating rate of 20°C/min from 40 to 600°C for MCMBs coalescence analysis. Thermal behaviors of MCMBs as received in air and nitrogen are observed through a polarized optical microscope (Leica-DMLP, Germany) with hot-stage. A heating rate is set at 15°C/min heating up to 400°C, then 5°C/min heating up to 550°C and maintaining for 5 min at 450°C, after that heating to 600°C by 15°C/min.

2.2. Cold molding and sintering

Taking 4 g of MCMBs without any binder in a mold (40 × 40 mm), it is pressed into a rectangular green plate of approximate 2 mm in thickness under different pressure from 70 MPa to 300 MPa respectively at ambient temperature. The plates are sintered in a horizontal tube vacuum furnace (under 3×10^{-2} Pa) at three different target temperatures of 800, 1150 and 1400°C. For all plates, the heating rate is the same of 5°C/min holding for 30 min at 600°C and for 1 h at the target temperature.

X-ray plate diffraction data (XRD) are collected through a Bruker-AXS D8 Advance apparatus for carbonized plates at 800, 1150 and 1400°C individually, provided with Cu 40 kV 40 mA radiation at 0.5 s/step of scanning speed.

2.3. Physical properties of carbon plates

The bulk densities of the green and the sintered plates are calculated by measuring volume and weight. Volume shrinkage and mass loss are calculated by the difference of the volume and the weight before and after carbonization to the volume and the weight of the carbonized plate respectively. The bulk open porosities of plates after carbonization are examined by Archimedes methods [19].

$$\theta_{\text{open}} = (w_2 - w_1)/(w_2 - w_3)$$

here θ_{open} is the open porosity of specimen, w_1 and w_3 are the weight of specimen in air and in distilled water respectively, and w_2 is the weight of the specimen after soaking in distilled boiling water for at least 4 h. Here the density of distilled water is supposed to be 1000 kg/m^3.

The bending strengths are measured by a three-point bending test with 25 mm span under a crosshead speed of 1.0 mm/min. Prior to testing, the carbonized spec-

imen is machined to a strip 6 mm wide. The bending strength, σ_b, is calculated by the equation:

$$\sigma_b = 3Pl/2wh^2$$

here P is the value of the load at failure, l is the distance between the fulcrums, w is the strip width and h is the strip thickness. The data are typically an average of three measurements in this paper.

The bulk electrical conductivities of carbonized plates are tested using a four-point probe technique and calculated by the following equation:

$$1/\rho = [I/V] \times [S/(hw)]$$

here I, V, S, h and w are the applied current, measured voltage, probe spacing, specimen thickness and width, respectively.

Morphologies of the fracture surface of carbonized plates are observed through a SEM (JEOL, JSM-840A).

3. Results and discussion
3.1. Morphology of MCMBs

Some individual researchers [11, 20–23] have described that mesophase spherules are a kind of nematic liquid crystal structure. Inside the spherules these planar polyaromatic molecules are arranged approximately parallel to each other and perpendicular to the surface. During heat treatment of mesophase pitches at temperatures between 350 and 500°C, polycondensed aromatic hydrocarbons are formed due to thermal decomposition and thermal polymerization reactions, followed by orientation of polycondensed aromatic hydrocarbons in a fixed direction. By the accumulation of oriented polycondensed aromatic hydrocarbons in layers, the mosophase spherule is formed. The Taylor lamellar structure model of a mesophase spherule is illustrated by Fig. 1. Fig. 2 is a SEM micrograph to show the morphology of mesophase spherules. Although there are other lamellar structure models [17, 23, 24] of mesophase spherules, Taylor's model is the most stable at the first heat stage [25].

3.2. Particle size and element analysis

MCMBs have significant self-sintering ability affected by many factors such as particle size, element composition, process pressure and sintering temperature. Obviously, these factors determine directly the properties of carbon plates after calcination. So the particle size and element composition of MCMBs should be taken
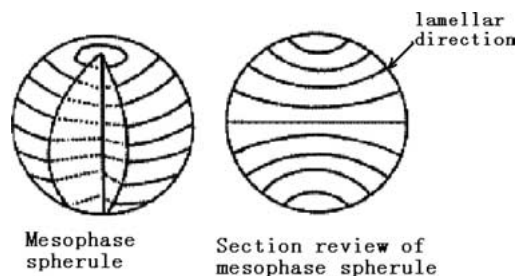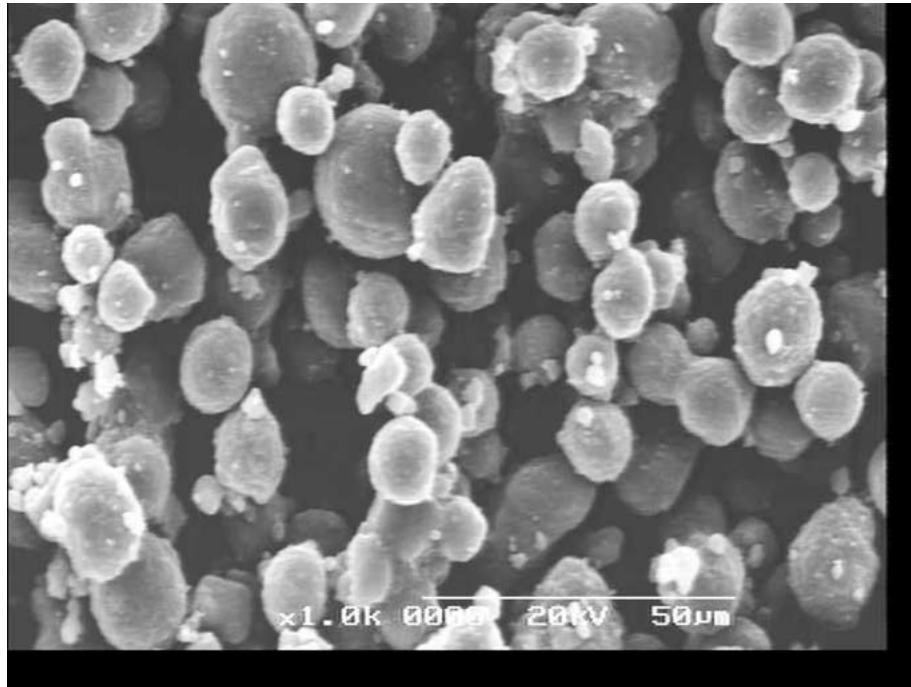

Figure 1 Taylor's model of MCMBs structure.

Figure 2 Morphology of as received MCMBs.

into account during process design. The driving force of sintering between particles derives from the decrease of surface energy of mesophase spherules. The smaller the particle size, the more favorable it is to sintering. Meanwhile it is also favorable for smaller particles size to form a homogenous green plate under pressure due to better flowability. But if particle size is too small, the disadvantage is that the smaller particles can easily cause cracking because of uneven distribution of thermal stress inside the carbon plate during sintering.
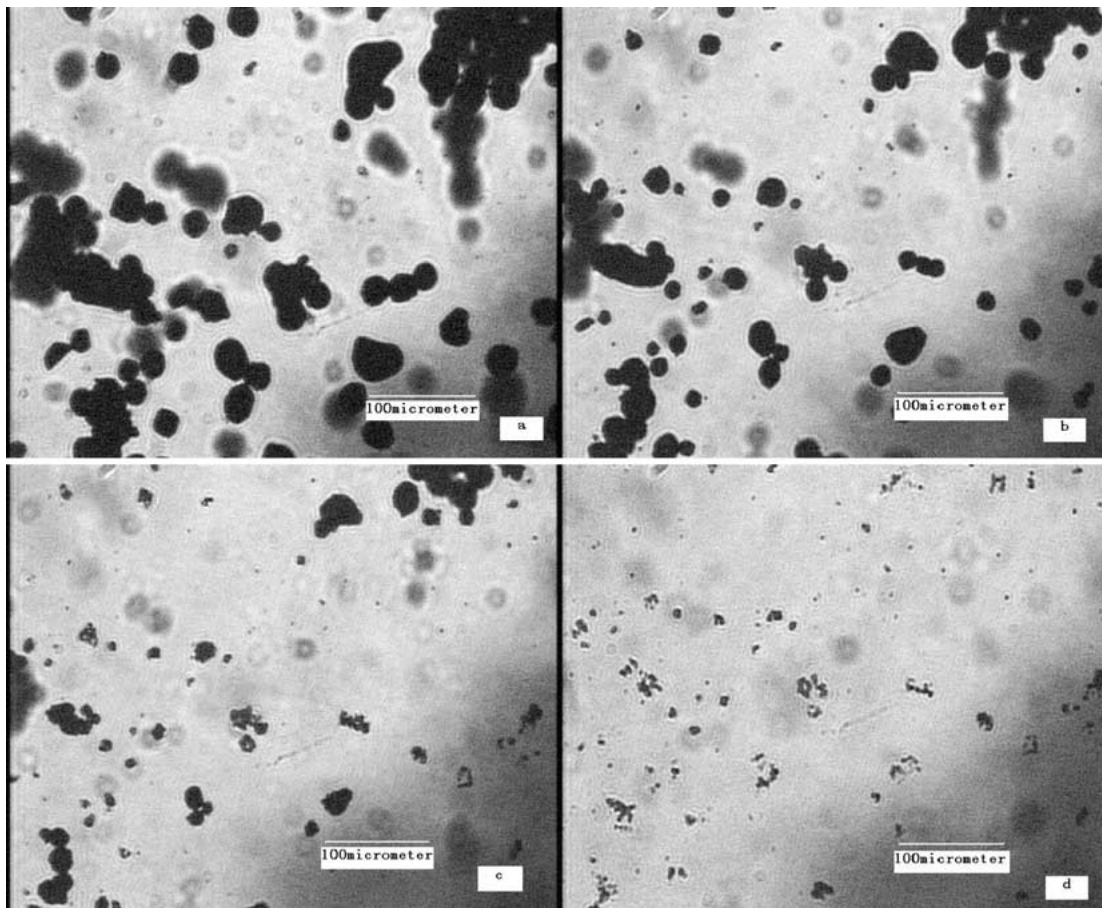
Figure 3 Optic micrograph photos with bright field: (a) at ambient temperature, (b) at 450°C, (c) at 500°C, and (d) at 600°C.

1737

TABLE I Elemental composition of MCMBs as received

Element	C	H	N	S	O	C/H mole ratio
Contents (wt%)	72.73	2.91	0.765	0.37	23.23	2.1

Moreover, the elemental composition is another important factor to affect sintering of MCMBs. It is believed that MCMBs are mainly comprised of polyaromatic molecules, but there are still some kinds of smaller molecules and some kinds of side chains on polyaromatic molecules which are relevant to self-sintering of MCMBs. The self-sintering of MCMBs can be roughly evaluated by the C/H mole ratio. The higher the C/N mole ratio is favorable for sintering in general. Table I presents the elemental composition of MCMB used in this experiment.

3.3. Thermal behaviors of MCMBs

Fig. 3a–d is the reflection polarized optical micrograph in bright field in nitrogen atmosphere which shows clearly changes of MCMBs observed by the same ap-
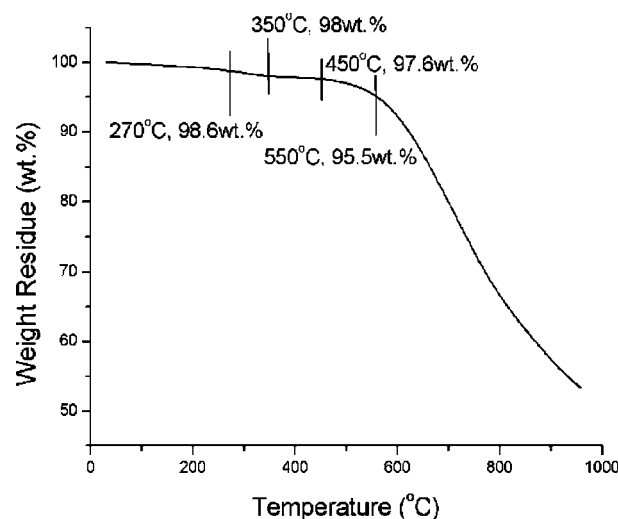

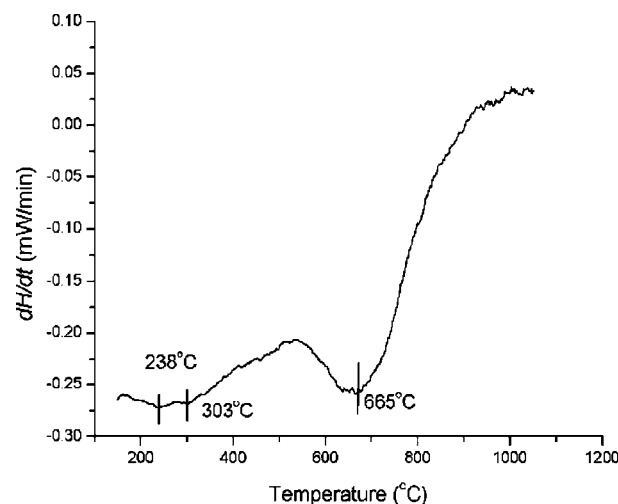*Figure 4* TG curve of MCMBs as received in nitrogen atmosphere.

Figure 5 DSC curve of MCMBs as received at a heating rate of 10°C/min from 40 to 1100°C.
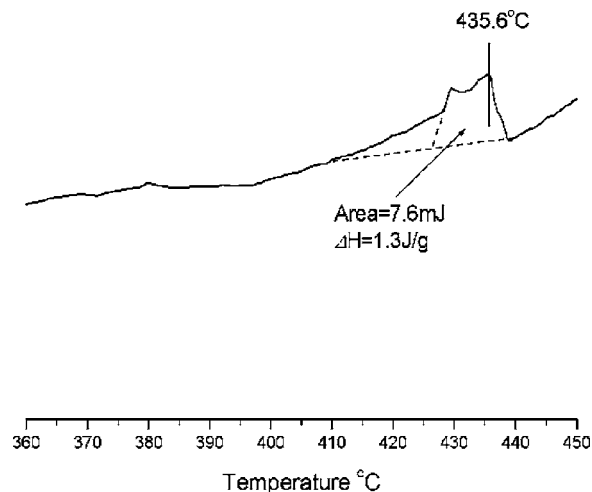

Figure 6 Magnified DSC curve of MCMBs as received in the interval from 360 to 450°C at a heating rate of 20°C/min.

paratus. A slight change of MCMBs is shown between Fig. 3a and indicating that partial fusion and pyrolysis of MCMBs occurs around 450°C, and a following distinct change between Fig. 3c and d reveals that the chemical reactions are intensive above 500°C.

Fig. 4 shows that MCMBs begin to lose weight slightly resulting from decomposition at approximately 270°C, followed by a plateau from 350 to 450°C. The subsequent intensive weight loss begins at 550°C lasting to 950°C. The endothermic peak at approximately 238°C in Fig. 5 indicates that some smaller molecules begin to be released because of decomposition. In Fig. 6, a slight exothermic peak at approximately 435°C indicates that the spherule coalescence occurs possibly due to the fusion of mesophase spherules or at least partial fusion on the particle surface, involving the polymerization and the condensation between active surface function groups or active side chains of MCMBs. Between 600 and 800°C in Fig. 5, there is a strong endothermic peak indicating that pyrolysis and dehydrogenation are very strong resulting in not only volatile release but also intensive volume shrinkage. The phenomenon extends up to 1100°C. So it is reasonable to infer that the coalescence and the formation of sintering bridges between spherules occur in the range of 435 to 550°C. It will be favorable for densification and graphitization of carbon plates if a slow heating rate is set between 435 and 550°C for coalescence and formation of sintering bridges of spherules, but a subsequent quick heating rate for gas release.

3.4. XRD of carbon plates

The lamellar arrangement of polyaromatic molecules of MCMBs determines directly the graphitization degree of carbon plates after calcination. The higher graphitization degree results in higher bulk density, better conductivity and higher bending strength. High heat treatment temperature is essential for graphitization, but the molecules arrangement of the precursors is of even more importance. Fig. 7 shows the graphitization
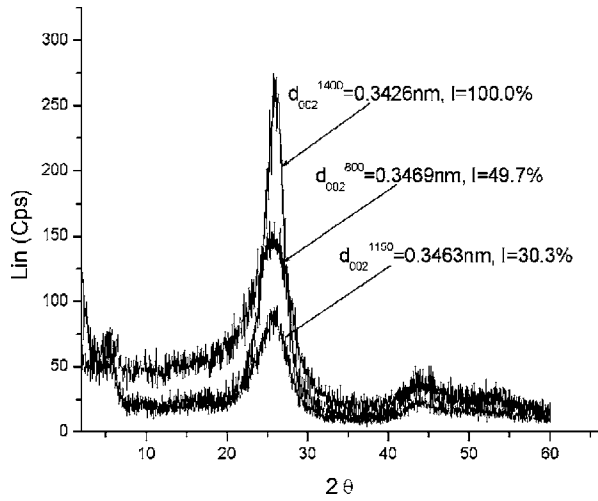
Figure 7 XRD diffraction patterns of carbon plates.

degree of carbon plates increasing and d_{002} decreasing from 0.3469 nm at 800°C to 0.3426 nm at 1400°C respecitively. d_{002} is the graphite interlayer spacing and I is the X-ray diffraction intensity defined relative to I = 100% at 1400°C.
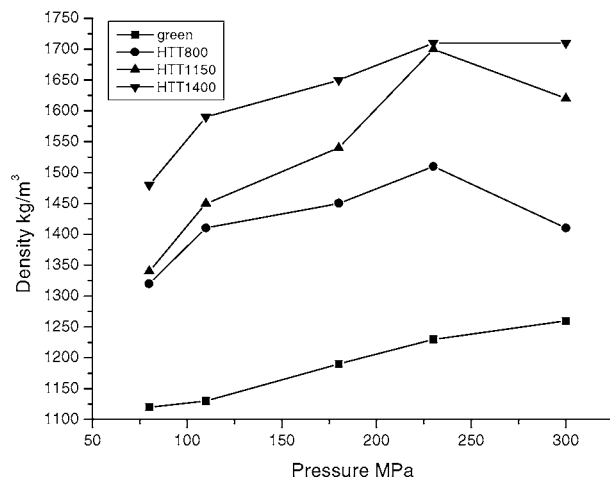

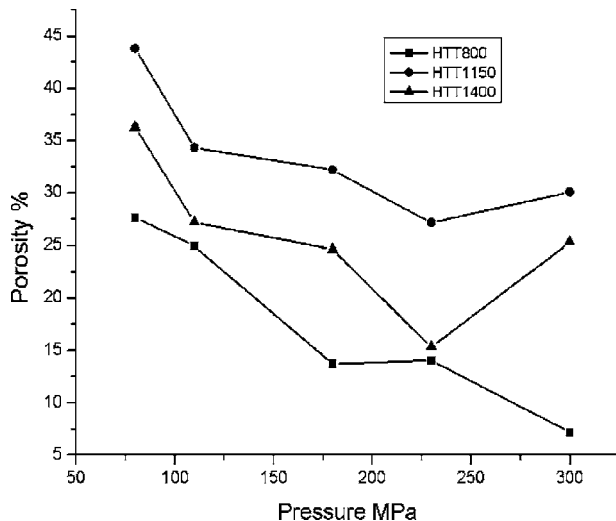Figure 8 The influence of process pressure and temperature on bulk density.

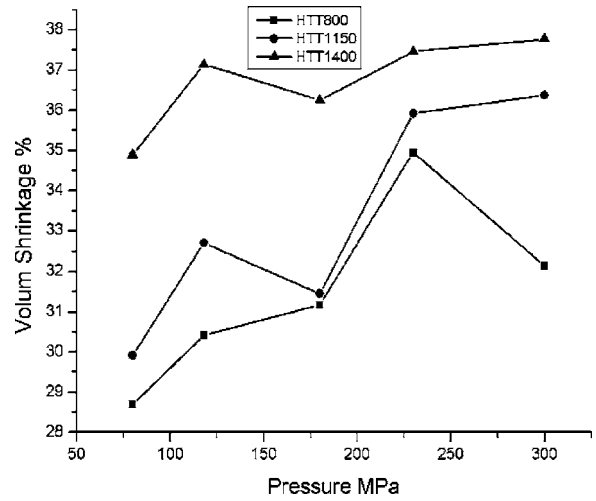Figure 9 The influence of process pressure and temperature on open porosity.

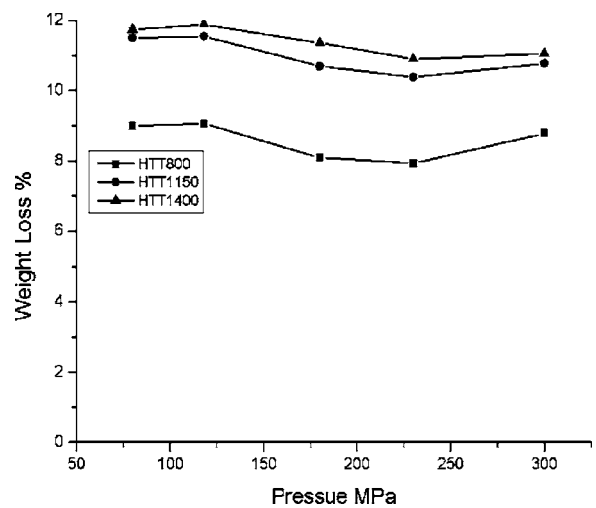Figure 10 The influence of process pressure and temperature on volume shrinkage.

Figure 11 The influence of process pressure and temperature on weight loss.
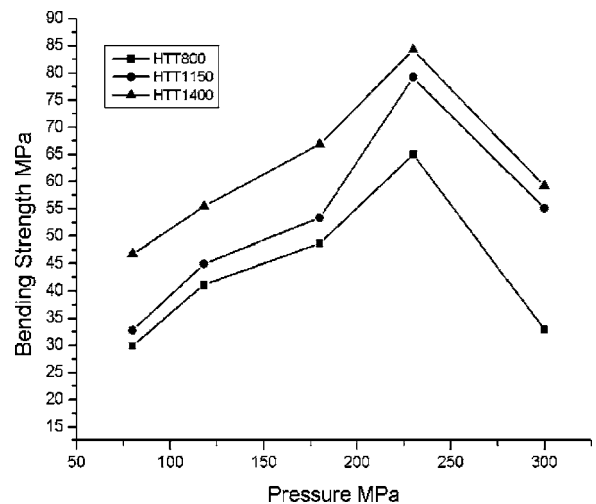

Figure 12 The influence of process pressure and temperature on bending strength.

3.5. Physical properties of carbon plates

It is clear from Figs 8–13 that the physical properties of the carbon plates are affected by the heat treatment temperature (HTT) and the process pressure. With
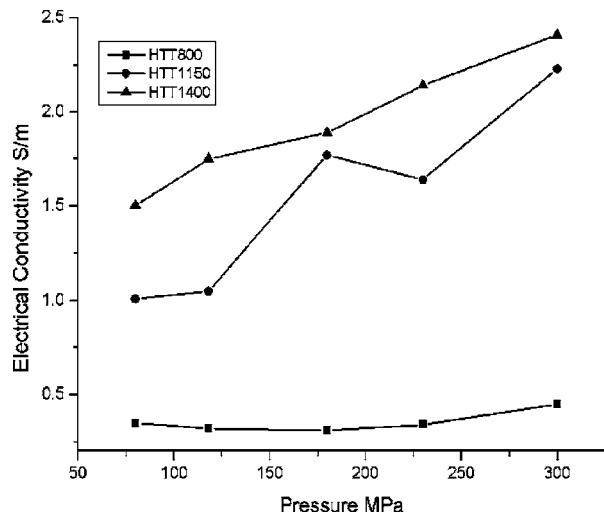
Figure 13 The influence of process pressure and temperature on electrical conductivity.

process pressure and HTT rising, the bulk densities of both green and sintered plates are increased from 1120 and 1320 kg/m^3 at 800°C and 80 MPa to 1260 and 1710 kg/m^3 at 1400°C and 300 MPa respectively, the bending strengths and the electrical conductivities also increase in all cases. The best results are the highest bending strength of 84 MPa at 1400°C and 230 MPa and the highest electrical conductivity of 2.4 S/m at 1400°C and 300 MPa, respectively. However, for the specimens at 800°C, Fig. 13 shows that the electrical conductivity has no obvious change with variation of process pressure because of insufficient carbonization. As for open porosity, volume shrinkage and weight loss, the trends are increscent with HTT rising, specially for weight loss in Fig. 11, the change is very remarkable between 800 and 1150°C but indistinct between 1150 and 1400°C which is in consistent with the previous thermal analysis. On the other hand, with pressure rising, the variations of properties are different. For all three cases at different temperature, the higher process pressure causes the lower porosity and the higher volume shrinkage, but the influence of pressure variation on weight loss is unapparent shown by Fig. 11. Furthermore, it should be noted that excessive pressure is harmful for the performance of carbon plates such as 300 MPa, the reason is possible that the excessive pressure causes more crackles produced during green body compressed. So the changes for all properties of carbon plates excluding electrical conductivity are abnormal under 300 MPa.

Fig. 14a, b and c shows the fractured surface of carbon plates after measurement of bending strength. These carbon plates are molded under 180 MPa and sintered at 800, 1150 and 1400°C respectively. It is observed that the boundaries between spherules disappear in all three photos, which means coalescence of MCMBs very well. The increase of sintering temperature delivers an improvement to the bending strength of carbon plates from 49 to 67 MPa.
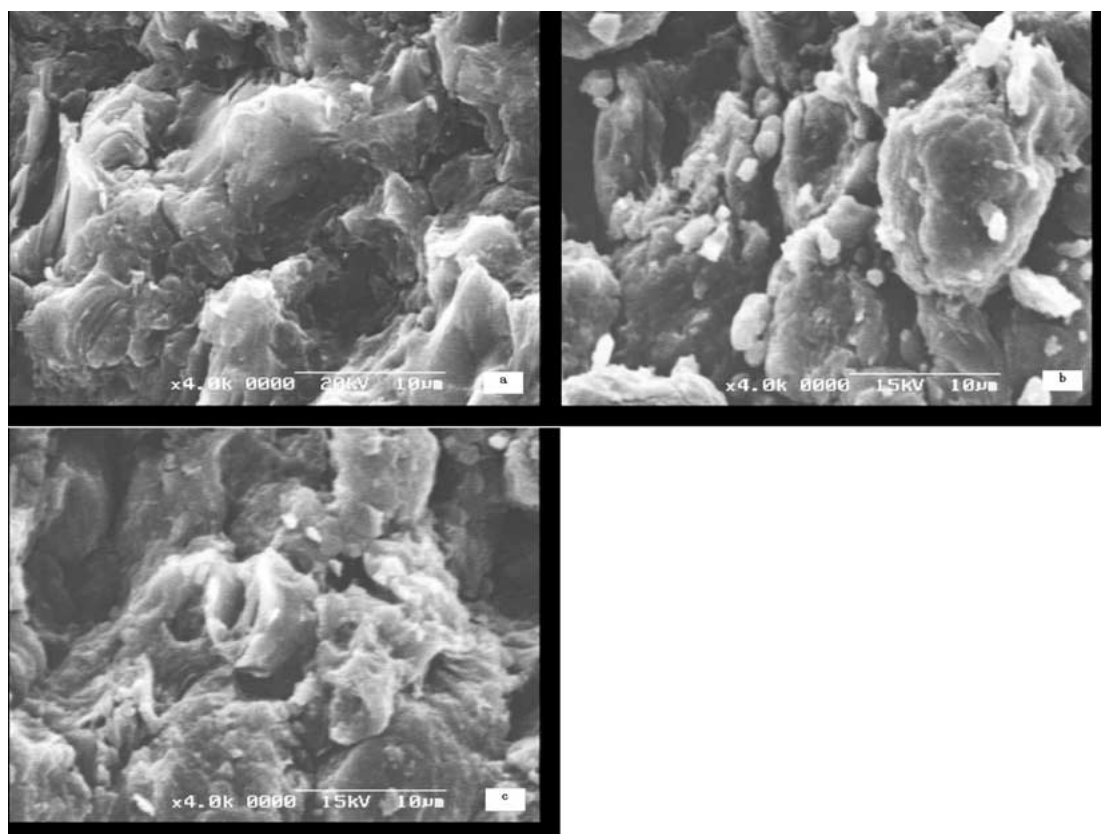

Figure 14 SEM photographs of the fractured surfaces of the carbon plates at carbonization temperature of (a) 800°C, (b) 1150°C, and (c) 1400°C with 180 MPa of compressed pressure.

1740

4. Conclusions

It is clear that MCMBs are a significant precursor for carbon artifacts without any binder and easy to be made into carbon plates with high density and high strength by cold molding. The sintering mechanism of MCMBs is an enhanced liquid-phase sintering between 435 and 550°C following intensive solidification shrinkage during a subsequent solid-phase carbonization. The driving force for sintering derives from the surface energy of the MCMBs, making spherules have a strong tendency to coalesce.

The present results reveal that process pressure is an important factor affecting bulk density, porosity and physical performances of the carbon plates. For preparation of carbon artifacts with high density and high strength, it always is possible to raise the process pressure to decrease porosity and increase bending strength, but excessive process pressure will cause crack to appear, thus decreasing bending strength in turn.

For optimizing sintering temperature, it is concluded that increasing temperature is favorable to improve bending strength and conductivity of carbon plates. The reason is that high temperature provides more energy for densification, rearrangement and dehydrogenation of polyaromatic molecules, and as a consequence, the carbonization and graphitization is more complete and the carbon plates display higher performance.

References

1. H. HONDA and Y. YAMADA, *J. Japan. Petrol. Inst.* **16** (1973) 392.
2. Y. WANG, Y. KORAI and I. MOCHIDA, *Carbon* **37** (1999) 1049.
3. R. FUJIURA, T. KOJIMA, M. KOMATSU and I. MOCHIDA, *ibid.* **33** (1995) 1061.
4. I. MOCHIDA, R. FUJIURA, T. KOJIMA, H. SAKAMOTO and T. YOSHIMURA, *ibid.* **33** (1995) 265.
5. Y. YMADA, K. SHIBATA, H. HONDA and S. OI, *Tanso* **88** (1977) 2.
6. N. FUKUDA and K. NAGASAWA, United States Patent no. 4,637,906.
7. N. OGATA, *Kogyozairyo* **27** (1979) 94.
8. R. K. AGGARWAL, G. BHATIA, O. P. BAHL and N. PUNJABI, *J. Mater. Sci.* **35** (2000) 5437.
9. Y. LU, L. LING, D. WU, L. LIU and B. ZHANG, *ibid.* **24** (1999) 4043.
10. M. MARTINEZ-ESCANDELL, P. CARREIRA, M. A. RODRIGUEZ-VALERO and F. RODRIGUEZ-REINOSO, *Carbon* **37** (1999) 1662.
11. H. HONDA, *ibid.* **26** (1988) 139.
12. W. R. HOFFMANN and K. J. HUTTINGER, *ibid.* **31** (1993) 259.
13. Y. YAMADA, T. IMAMURA, H. KAKIYAMA, H. HONDA, S. OI and K. FUKUDA, *ibid.* **12** (1974) 307.
14. W. R. HOFFMANN and K. J. HUTTINGER, *ibid.* **31** (1993) 263.
15. Y. G. WANG, M. EGASHIRA, S. ISHIDA, Y. KORAI and I. MOCHIDA, *ibid.* **37** (1998) 307.
16. W. R. HOFFMANN and K. J. HUTTINGER, *ibid.* **32** (1994) 1087.
17. H. FUJIMOTO and M. SHIRAISHI, *ibid.* **39** (2001) 1753.
18. P. HARIDOSS, F. A. URIBE, F. H. GARZON and T. A. ZAWODZINSKI, JR., *J. Mater. Res.* **13** (1998) 2015.
19. R. MORREL, "Handbook of Properties, Technical and Engineering Ceramic", (NPL, 1986) Part 1.
20. M. KODAMA, T. FUJIURA, E. IKAWA, K. ESUMI, K. MEGURO and H. HONDA, *Carbon* **29** (1991) 43.
21. S. H. YOON, Y. D. PARK and I. MOCHIDA, *ibid.* **30** (1992) 781.
22. I. MOCHIDA, Y. KORAI, C. H. KU, F. WATANABE and Y. SAKAI, *ibid.* **38** (2000) 305.
23. Y. KORAI, S. ISHIDA, S. H. YOON, Y. G. WANG, I. MOCHIDA, Y. NAKAGAWA, C. YAMAGUCHI, Y. MATSUMURA, Y. SAKAI and M. KOMATU, *ibid.* **35** (1997) 1503.
24. I. MOCHIDA, K. MAEDA and K. TAKESHITA, *ibid.* **16** (1978) 459.
25. J. D. BROOKS and G. H. TAYLOR, *ibid.* **3** (1965) 185.